

Half-Cycle Pulse Assisted Electron-Ion Recombination

T. J. Bensky, M. B. Campbell, and R. R. Jones

Department of Physics, University of Virginia, Charlottesville, Virginia 22901

Unipolar “half-cycle” electric field pulses (HCPs) have been used to recombine free electrons and calcium ions. The field assisted process is very similar to controlled three-body recombination in plasmas. We report on experiments that utilize HCP assisted recombination to probe the probability distribution of continuum electron wave packets and produce bound wave packets that are highly localized in three spatial dimensions.

The combination of free electrons and ions to form neutral atoms is a complicated process that can proceed through a variety of different mechanisms including di-electronic, radiative, or three-body recombination [1]. Although these mechanisms are quite different in detail, in general, recombination is made possible through the transfer of energy and momentum from the free electron to a third body. The recombination process is inherently time dependent, and the capture of a free electron can result in the formation of a complicated coherent superposition state within each atom. Because of the random nature of electron-ion scattering events in the laboratory, the bound wave packet produced via recombination varies widely from one atom to another due to the different scattering conditions through which each was formed. Consequently, standard theoretical and experimental studies parametrize the process using time-independent recombination rates and branching ratios for capture into various excited states of the atom [1].

The experiments described in this Letter are aimed at studying controlled electron-ion recombination in the time domain. The results of these experiments provide new information on coherent recombination processes as well as demonstrate the utility of field assisted recombination for probing continuum electron dynamics and producing novel bound wave packets. Specifically, subpicosecond “half-cycle” field pulses (HCPs) [2,3] have been used to assist the recombination of a well-characterized continuum wave packet with its parent ion. Although the recombination can be formally classified as radiatively assisted [1], the unique nature of the unipolar field pulse makes the process more closely related to three-body recombination. To make the analogy with three-body recombination the HCP field is equated with the transverse field produced by a passing ion or electron. The impulse provided by the field [4,5] extracts momentum and energy from the free electron, facilitating its capture by an ion.

In the experiments, a 1.5 psec laser pulse photoionizes a tightly bound electron in calcium, producing a continuum wave packet which travels away from the Ca^+ ion in the form of a thin shell. After the ionizing laser pulse, the ions and free electrons are exposed to a HCP whose duration is so short that the continuum wave packet is

essentially frozen during the pulse. The electron receives a momentum “kick” or impulse, $\vec{A} = - \int \vec{F}_{\text{HCP}}(t) dt$, from the HCP [4,5], where $\vec{F}_{\text{HCP}}(t)$ is the HCP field amplitude. All equations are given in atomic units unless otherwise noted. The impulse can halt or sufficiently slow the expansion of the continuum wave packet on one side of the ion, producing a *bound* Rydberg wave packet. The dynamics of the recombination process are studied by monitoring the production of bound Rydberg states as a function of the wavelength of the ionizing picosecond laser, the HCP field amplitude, the HCP polarization, and the relative delay between the ionizing laser and the HCP. These experimental parameters correspond to the physically interesting variables: continuum electron energy, kick amplitude, kick direction, and wave packet radius, respectively.

The experiments take place in a vacuum chamber with a background pressure of 10^{-6} Torr. The lasers and HCP interact with a low density thermal calcium beam ($\approx 10^9$ atoms/cm³) between two parallel aluminum capacitor plates. The $4s4s\ ^1S_0$ ground state Ca atoms are excited to an intermediate $4s4p\ ^1P_1$ level using a 423 nm, 5 nsec dye laser pulse before being photoionized near threshold by a 390 nm, 1.5 psec laser pulse. The 1.5 psec pulse is generated by frequency doubling the 120 fsec, 786 nm output from an amplified Ti:sapphire laser in a 3 cm long potassium dihydrogen phosphate (KDP) crystal. Phase-matching effects restrict the bandwidth of the doubled light, producing a 1.5 psec pulse that can be continuously tuned from 390 nm to 394 nm by varying the angle of incidence into the KDP crystal. Both laser pulses are linearly polarized in the same direction, producing a predominantly $4s\epsilon d, m_\ell = 0$ wave packet.

After the launch of the continuum wave packet, the free electrons and ions are exposed to a subpicosecond unipolar field pulse which is generated by gating a biased, large-aperture GaAs photoconductive switch [2] with a 786 nm, 120 fsec laser pulse. The HCP is linearly polarized along the bias field axis, and its field amplitude is proportional to the bias voltage [2]. Small nonunipolar features are removed from the HCP using a second, gated GaAs wafer as a transient attenuator [2,6]. Approximately 20 nsec after the HCP a +50 V pulse is applied

to the upper capacitor plate, pushing any remaining ions toward the lower capacitor plate. After several microseconds a +2.5 kV pulse is applied to the lower plate, field ionizing the neutral Rydberg atoms formed via HCP assisted recombination. Ions created by the field ionization pulse are accelerated through a 2.5 cm \times 0.15 cm slit in the upper capacitor plate towards a microchannel plate detector.

Using a delay imaging detector, it is possible to monitor the recombination process over a range of delays, τ , between the HCP and ionizing laser (i.e., wave packet radii) in a single laser shot [7]. The detector exploits a crossed beam geometry to generate a delay sweep between the HCP and laser beams beneath the extraction slit. The recombination signal as a function of τ is directly related to the field ionization signal as a function of position along the extraction slit.

Figure 1 shows a density plot of the measured recombination signal for a wave packet with total energy $E \approx 25 \text{ cm}^{-1}$ as a function of HCP impulse and delay. The maximum recombination probability is on the order of a few percent. The inset of Fig. 1 shows a polar plot of the recombination signal as a function of the angle between the HCP and laser polarizations which closely resembles the expected d -wave distribution. The data in the inset are obtained with the HCP amplitude and delay fixed near the maximum in the density plot. Clearly, HCP assisted recombination provides a method for determining the angular distribution of continuum wave packets with energies $\approx 1 \text{ meV}$.

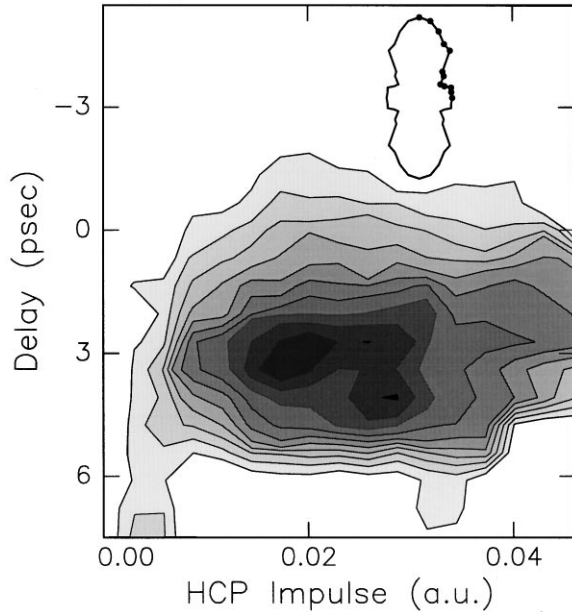


FIG. 1. Density contour plot of HCP assisted recombination probability as a function of HCP impulse and delay relative to the creation of the $E \approx 25 \text{ cm}^{-1}$ continuum wave packet. The dark area indicates high probability. The inset polar plot shows the recombination probability as a function of the relative angle between the HCP and ionizing laser pulse.

The limited range of HCP kick magnitudes and continuum wave packet radii which produces measurable recombination can be understood as follows. If the HCP is too weak, insufficient momentum is extracted from the wave packet to cause recombination. Conversely, strong kicks can actually reverse the velocity of part of the wave packet, sending the electron back towards the ion as a continuum rather than bound packet. The 2 psec rise of the recombination signal near $\tau = 0$ is the convolution of the 1.5 psec laser pulse and the $\approx 1 \text{ psec}$ HCP. The rapid decrease in the recombination signal for $\tau > 5 \text{ psec}$ is due to the 50 V clearing pulse. In the impulse approximation, recombination can occur only to states whose wave functions have non-negligible overlap with the continuum packet. Approximately 6 psec after the wave packet is launched, its radius has become so great that recombination can only occur to high n states that are field ionized directly by the clearing pulse and, therefore, are not detected [8].

It is interesting to consider the dynamics of the bound wave packet that is formed as the result of the recombination process. Figure 2 shows the evolution of a classical ensemble of electrons ejected from the ion core at $t = 0$. The ensemble has a mean energy equal to its 30 cm^{-1} bandwidth, $\ell = 2, m_\ell = 0$, and is ejected into a 4π solid angle. A two-dimensional image of the probability distribution is produced by integrating the angular distribution over the azimuthal angle ϕ . After 10 psec (Fig. 2A), the ensemble is given a HCP impulse in the $+z$ direction. The impulse does not alter the expansion of the wave packet about its center of gravity, but instead it gives the wave packet center a velocity relative to the parent ion (Fig. 2B). The portion of the ensemble initially moving in the $-z$ direction is effectively stopped by the kick and this recombined fraction subsequently accelerates back towards the parent ion. After 50 psec (Fig. 2C), both the bound and continuum parts of the ensemble are so broadly dispersed that they are virtually invisible on the amplitude scale of Fig. 2. Surprisingly, after 70 psec,

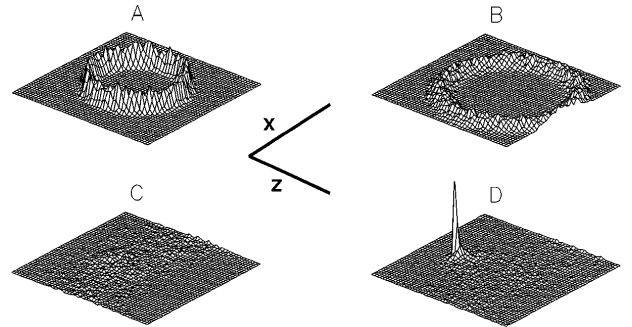


FIG. 2. Results of a classical simulation of the evolution of a radial continuum wave packet that is kicked by a HCP as described in the text. The wave packet is kicked 10 psec after it is launched, and its spatial distribution is shown after (A) 10 psec, (B) 15 psec, (C) 47 psec, and (D) 72 psec. The axis scales are identical in each frame with x and z running from $-20\,000$ to $+20\,000$ a.u. and the y scale in arbitrary units.

the bound “wave packet” collapses to a single probability spike localized in three dimensions (Fig. 2D). This “return” of the bound wave packet to its birth place lasts for approximately 20 psec or so before dispersing. The radial position and angular orientation of the probability spike are determined by the HCP delay and polarization direction. Therefore, the simulation suggests that we are producing these nearly classical electron packets in the laboratory, and that we can control their characteristics for use in future experiments.

HCP assisted recombination can also be used as a probe of continuum electron dynamics. Consider a classical electron with positive energy δ and momentum \vec{p} which receives a sudden momentum kick, $\vec{A} = -A\hat{n}$, $A > 0$. The electron experiences a change in its total energy [4,5], $\Delta E = \vec{p} \cdot \vec{A} + A^2/2$ due to the impulse and will recombine with a nearby positive ion if $\Delta E \leq -\delta$. This occurs whenever $p_n \equiv \vec{p} \cdot \hat{n} \geq A/2 + \delta/A \equiv p_{\text{crit}}$. Therefore, the recombination probability for a wave packet is equal to the probability that the electron has a momentum projection, $p_n \geq p_{\text{crit}}$. By measuring the recombination signal as a function of delay and HCP field, one can recover a portion of the wave packet’s time-dependent momentum space probability distribution [9]. This technique is essentially the inverse of impulsive momentum retrieval, where the momentum distribution of a bound wave packet is determined through HCP ionization [5].

HCP assisted recombination has been used to study the dynamics of wave packets in a static field induced continuum in Ca. The experiment proceeds in a manner which is nearly identical to the field free experiment. However, the atoms are excited to a wave packet with negative total energy $-E_c + \delta < 0$ in the presence of a static electric field F_s . The static field induces a saddle point at energy $-E_c = -2\sqrt{F_s}$ in the binding potential and replaces the 50 V clearing pulse. Since lowering the energy of an electron when it is outside the saddle point traps it in the continuum part of the potential, HCP assisted recombination provides a view of the momentum of a Stark continuum wave packet *before* it passes over the saddle point, in contrast to an atomic streak camera [10] which determines *when* a wave packet passes over the saddle point.

Examples of time-dependent recombination measurements are shown in Fig. 3 for a wave packet with a mean principal quantum number $\bar{n} = 42$ in a static field $F_s = 212$ V/cm, approximately twice the critical field, $F_c = n^{-4}/16$, required to ionize an $n = 42$, $m_\ell = 0$ level. Figure 3A shows the recombination probability for \vec{F}_{HCP} oriented antiparallel to F_s (negative HCP), while Fig. 3B shows the analogous signal for parallel fields (positive HCP). The curves in Fig. 3 are representative in that they show several general features of data taken at a variety of different static fields with wave packets having different values of \bar{n} . First, for small delays we observe relatively high recombination probabilities, on the order of 10%–15%. Second, the recombination signal shows pronounced modulations at the classical Kepler

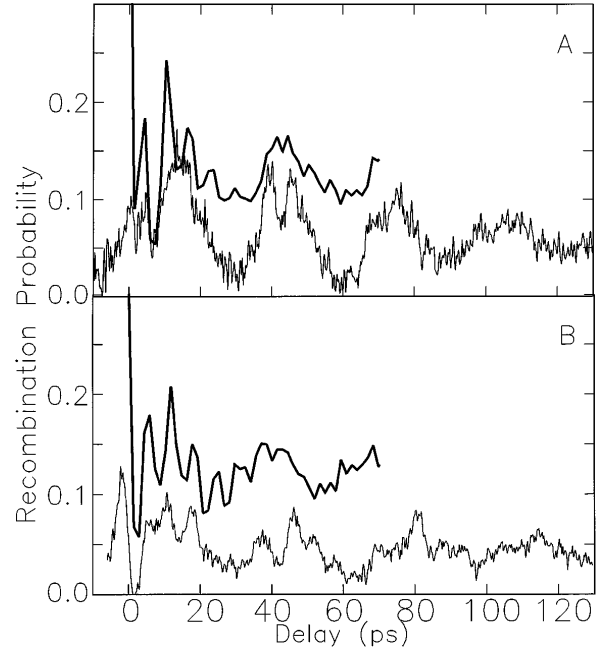


FIG. 3. HCP assisted recombination of $\bar{n} = 42$ wave packets in a 212 V/cm static electric field induced continuum as a function of the delay between the launch of the wave packet and the HCP kick. (A) This shows the recombination probability for antiparallel HCP and static fields (negative HCP) while (B) shows corresponding data for parallel fields (positive HCP). The bold lines shown with the data are the results of the classical simulation described in the text and are offset vertically by 0.05.

period $\tau_K = 2\pi\bar{n}^3$ ($\tau_K = 11$ psec for $\bar{n} = 42$) if the HCP and static field have the same polarization axis. For orthogonal polarizations, no oscillations at the Kepler period are observed. Third, strong modulations at the angular momentum precession or Stark period $\tau_S = 2\pi/3F_s\bar{n}$ ($=28$ psec for the conditions of Fig. 3) are seen irrespective of the polarization direction of the HCP field. However, the phase of the Stark oscillation changes with the relative polarization of the HCP and static fields. Last, significant recombination occurs for delays of hundreds of picoseconds when $F_s \approx F_c$ showing explicitly that ionization (i.e., passage over the saddle point) is not immediate even for a wave packet with energy $E \geq -E_c$. This observation is understood by recalling that, for $F_s \approx F_c$, the escape “hole” in the binding potential spans only a small solid angle. Consequently, only a small part of the wave packet encounters the saddle point at any given time. Rapid ionization occurs in larger static fields, where the hole in the potential is much larger and harder to miss. Static fields on the order of 3 times the critical field are required to guarantee ionization in one Stark period or so.

A full quantum simulation of wave packet dynamics in nonhydrogenic atoms in strong static fields [11] is beyond the scope of this paper. Indeed, an important feature of the experimental method is that it provides a means for direct measurement of wave packet dynamics in systems

that cannot be easily modeled quantum mechanically. However, it is instructive to treat the system classically to identify any inherently classical features in the wave packet evolution as well as provide insight into the specific features of the time-dependent recombination signal.

To this end, the classical equations of motion for an ensemble of electrons in a combined Coulomb and Stark potential are numerically integrated. The ensemble is launched from the inner turning point of a hydrogenic $\ell = 2, m_\ell = 0$ orbit into a 4π solid angle. Since the wave packet created in the experiment resembles a radial wave packet [12] consisting of approximately eight d states with $39 \leq n \leq 46$, the elements of the classical ensemble are given discrete energies and angular momenta to reproduce the experimental conditions at $t = 0$. After some time, the ensemble is exposed to a 1 psec Gaussian HCP, and the energy and location of each electron in the ensemble is evaluated. Any electron located inside the saddle point, with an energy $E < -E_c$ after the pulse has undergone recombination.

The results of the classical simulation for $\bar{n} = 42$ in a static field of 212 V/cm are shown along with the data in Fig. 3. For short times ($\tau < 30$ psec) there is good qualitative agreement between the experiment and theory. Therefore, it seems reasonable to use the insight gleaned from the classical simulation to aid our interpretation of the differences in the data presented in Figs. 3A and 3B. Near $\tau = 0$, the wave packet expands radially, essentially unaffected by the static field. Positive (negative) HCPs are equally likely to recombine portions of the wave packet moving in the “uphill” (“downhill”) direction, and a large recombination peak is visible for both polarities. However, after 2 psec or so, the mean radius of the wave packet has increased significantly, greatly reducing the recombination probability for both HCP polarities. The uphill part of the wave packet reflects from the binding potential at $\tau = 4$ psec and travels downhill toward the ion. The reflected part of the packet can then be recombined by the negative HCP, producing the second peak in Fig. 3A at $\approx 1/2$ the Kepler period. No analogous peak is seen in Fig. 3B since the portion of the wave packet initially traveling downhill passes over the saddle point and never reverses its direction of travel. The subsequent Kepler oscillations in both data sets correspond to “radial” motion purely on the uphill side of the potential. The slower Stark beats are produced by the precessional motion of quasi-closed orbits in the static field. A full description of the classical dynamics and our detailed measurements will be presented in another article. While the simulation provides valuable insight into the wave packet dynamics responsible for the structure observed early in the continuum packet’s evolution, the effects of quantum phase and the nonhydrogenic core become more important at longer times, and the classical approach fails to provide even qualitative agreement with the data.

As stated above, no radial oscillations are observed with perpendicular HCP field configurations. This is further

confirmation of the classical prediction that radial oscillations only occur on the uphill side of the potential, a motion that does not strongly influence the momentum distribution along any perpendicular axis. However, the perpendicular case is complicated by the fact that m_ℓ redistribution during the HCP kick also causes recombination. Roughly speaking, the HCP can kick the electron off to the side so that its trajectory misses the saddle point in the potential. In general, it appears that HCP assisted recombination in the presence of a static field can be more efficient for perpendicular orientations. We plan to study this effect in detail in the future.

In summary, we have demonstrated HCP assisted, coherent recombination of well-characterized free electron wave packets and ions. The recombination process has been used to produce bound wave packets localized in three dimensions as well as probe the momentum and spatial distribution of continuum wave packets.

We gratefully acknowledge the support of the AFOSR and the Packard Foundation.

- [1] Yukap Hahn, Rep. Prog. Phys. **60**, 691 (1997), and references therein; R. Flannery, *Atomic, Molecular, and Optical Physics Handbook* (AIP Press, Woodbury, NY, 1996), p. 52.
- [2] D. You *et al.*, Opt. Lett. **18**, 290 (1993).
- [3] R.R. Jones, D. You, and P.H. Bucksbaum, Phys. Rev. Lett. **70**, 1236 (1993).
- [4] C.O. Reinhold *et al.*, J. Phys. B **26**, L659 (1993); C.O. Reinhold, H. Shao, and J. Burgdorfer, *ibid.* **27**, L469 (1994); A. Bugacov *et al.*, Phys. Rev. A **51**, 1490 (1995); P. Krstic and Y. Hahn, *ibid.* **50**, 4629 (1994).
- [5] R.R. Jones, Phys. Rev. Lett. **76**, 3927 (1996); C. Raman *et al.*, *ibid.* **76**, 2436 (1996); C.O. Reinhold *et al.*, Phys. Rev. A **54**, R33 (1996).
- [6] N.E. Tielking, T.J. Bensity, and R.R. Jones, Phys. Rev. A **51**, 3370 (1995).
- [7] M.B. Campbell, T.J. Bensity, and R.R. Jones, Opt. Express **1**, 197 (1997).
- [8] Through similar reasoning, recombination to very high n states should be observable for HCPs with nanosecond durations such as those used by M.T. Frey *et al.*, Phys. Rev. A **53**, R2929 (1996), and P. Kristensen *et al.*, J. Phys. B **30**, 1481 (1997).
- [9] The minimum absolute value of p_n that can lead to recombination is $p_{\min} = \sqrt{2\delta}$, so reconstruction of the momentum distribution for $|p_n| < p_{\min}$ is not possible. Maximum recombination occurs when the impulse $A = \sqrt{2\delta}$, independent of the radius of the wave packet, providing an experimental method for measuring the mean energy of the wave packet.
- [10] G.M. Lankhuijzen and L.D. Noordam, Phys. Rev. Lett. **76**, 1784 (1996).
- [11] F. Robicheaux and J. Shaw, Phys. Rev. Lett. **77**, 4154 (1996).
- [12] J. Parker and C.R. Stroud, Phys. Rev. Lett. **56**, 716 (1986); A. ten Wolde *et al.*, *ibid.* **61**, 2099 (1988).